Spine

SPINE Volume 42, Number 21, pp 1604–1613

BASIC SCIENCE

Posterolateral Disc Prolapse in Flexion Initiated by Lateral Inner Annular Failure

An Investigation of the Herniation Pathway

Vonne M. van Heeswijk, MSc,* Ashvin Thambyah, PhD,* Peter A. Robertson, MD,† and Neil D. Broom, PhD*

Study Design. Structural investigation of mechanically induced herniations in ovine lumbar motion segments.

Objective. This new study addresses the question of whether there are regions other than the posterior and posterolateral aspects that are implicated in the initiation of disc disruption and herniation.

Summary of Background Data. Flexion in combination with compressive loading will induce disc herniations in healthy motion segments *in vitro*. Although it is widely accepted that the posterior and posterolateral regions of the disc are the primary sites of herniation much less is known as to whether other regions of the disc might be involved in the herniation process.

Methods. Healthy ovine lumbar motion segments (n = 14) were flexed 10° and compressed at a rate of 40 mm/min up to point of failure. The discs were macroscopically analyzed using progressive transverse sectioning to obtain a more global picture of internal disc disruption and herniation.

Results. A high prevalence of disruption in the lateral annulus was found associated with circumferential tracking of nucleus between the annular layers toward the posterolateral and posterior regions. In all tests this lateral disruption did not cause any discernible external change in the lateral disc periphery after the removal of load. After imposing the predetermined flexion the applied compression also induced a forward anterior shear of the superior vertebra of approximately equal magnitude to the axial compressive displacement.

Conclusion. The vulnerability of the lateral annulus to disruption is thought to arise from the overloading of its differentially recruited oblique/counteroblique fiber sets, this in turn generated by anterior shear developed in the flexed, compressed motion segment. This lateral annular disruption, followed by circumferential tracking of nuclear material and resulting in either contained or uncontained extrusions in the posterior or posterolateral annulus, highlights the complexity of the herniation process.

Key words: anterior shear, circumferential nuclear tracking, flexion and compression, herniation pathway, lateral annulus disruption, ovine lumbar motion segments, progressive transverse sectioning, structural analysis.

Level of Evidence: N/A

Spine 2017;42:1604–1613

Both internal disc disruption[1,2] and overt herniation cause low back pain by stimulating nerve endings[3–5] situated in the outer third of the disc.[4,6–8] When herniation occurs, either focal disc bulging or extrusion of nuclear material may irritate, inflame, and/or compress the adjacent nerve roots causing sciatica.[9]

In vitro cadaver studies have shown that compressing discs in flexion increases the likelihood of herniation,[10–12] whereas compression of the disc in its neutral posture almost invariably leads to vertebral endplate failure.[13–15] Previous *in vitro* studies using ovine lumbar discs have shown that it is possible to induce herniations using a novel internal pressurization technique.[16–19] Although nonphysiological, these ovine studies did highlight the potential importance of both loading rate and posture on disc disruption and herniation.

More recently Wade *et al*[20,21] investigated the influence of loading rate and posture by compressing intact ovine lumbar motion segments under conditions much more akin to *in vivo* function. Their studies showed that to achieve herniations a flexed posture of 10° and a minimum compressive rate of 40 mm/min was required. The same flexion but with a lower compressive rate of 4 mm/min, or a neutral posture irrespective of rate, resulted in vertebral endplate failure. Furthermore, these investigators sagittally sectioned

From the *Experimental Tissue Mechanics Laboratory, Department of Chemical and Materials Engineering, University of Auckland, Auckland, New Zealand; and †Department of Orthopaedic Surgery, Auckland City Hospital, Auckland, New Zealand.

Acknowledgment date: December 21, 2016. First revision date: February 20, 2017. Acceptance date: March 17, 2017.

The manuscript submitted does not contain information about medical device(s)/drug(s).

Medtronic Australasia funds were received in support of this work.

Relevant financial activities outside the submitted work: consultancy.

Address correspondence and reprint requests to Neil D. Broom, PhD, Department of Chemical and Materials Engineering, University of Auckland, Private Bag 92019, Auckland, New Zealand;
E-mail: nd.broom@auckland.ac.nz

DOI: 10.1097/BRS.0000000000002181

their herniated discs to investigate microscopically the mechanism of annular wall/endplate failure, particularly focusing on the posterior and posterolateral aspects.[20]

Although it is generally accepted that the posterior and posterolateral regions of the disc are the primary herniation sites[22–25] *via* direct radial rupture of the annulus,[24,25] the question remains as to whether there are also mechanisms of herniation operating in other regions that do not necessarily involve direct radial rupture. We consider that this latter question is best addressed by employing a method of structural analysis able to capture evidence of any more globally distributed damage within the whole disc, and hence this new study.

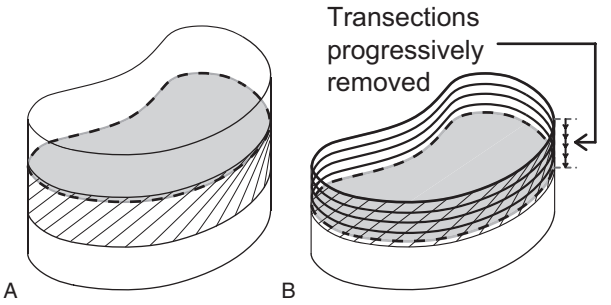

Figure 1. Schematic illustrating the progressive transverse sectioning method. **A**, The first transverse cut was made as close as possible to one of the vertebra followed by a progression of cuts (indicated with the small arrows) until the other vertebra was reached as shown in (**B**).

MATERIALS AND METHODS

Sample Preparation

Mature ovine lumbar spines (age 3–5 yr) were collected soon after sacrifice and stored at −28°C. Following thawing, extraneous tissues were removed from each lumbar spine and dissected into L1-L2, L3-L4, or L5-L6 motion segments. The facet joints were retained to restrict anterior shear to within physiological limits.[14,26–28] If inspection of any transected disc revealed an abnormality such as a rupture, focal disruption, or discoloration, then the total spine was discarded. Each motion segment was submerged in physiologic saline at 4°C for at least 20 hours to ensure a consistent level of hydration[29–31] and the vertebrae then mounted in metal cups using dental plaster.

Mechanical Testing

Using a custom-built rig[20,21] each motion segment was flexed 10° followed by axial compression at a rate of 40 mm/min up until detection of an audible fibrous tearing sound.[20] The tests were video recorded from the lateral view to capture the downward and forward displacements of the superior vertebra permitted by the freedom of forward motion of the upper portion of the rig, and to determine the load at initial failure. With SPSS software (version 23; IBM Corp., Armonk, NY) a one-way ANOVA was performed to test for a significant difference in mean initial failure load between the three spinal levels used. Mean initial failure loads from the present study and a previously published study[20] using the same ovine model and testing conditions was tested for significance with a *t* test.

Structural Analysis

The tested motion segments were chemically fixed (10% formalin) and decalcified (10% formic acid). After external examination of the disc the facet joints were carefully removed to enable transverse sectioning. Then a first cut was made transversely close to one of the vertebra (Figure 1A) followed by a progressive series of transverse cuts until the other vertebra was reached (Figure 1B). When the damage appeared less obvious the number of slices was increased by reducing their thickness to increase the level of structural resolution. On average approximately eight slices were taken from each motion segment with a thickness range from 0.3 to 0.9 mm and an average thickness of 0.5 mm. After each transverse cut both the exposed surface of the disc and the transectioned slice were systematically examined in their fully hydrated state with reflected light microscopy. The sections were always orientated for imaging such that the anterior of the disc was uppermost, a small schematic is included in images where appropriate. The microscopy was coupled with gentle physical probing to help differentiate between annulus and nuclear material where they had become intermingled.

Sample Numbers

A total of 14 motion segments from 12 ovine lumbar spines were assigned to the present study with no particular preference given to a particular spinal level. All remaining segments were employed for other unrelated studies. Two other segments that were tested suffered endplate fracture but were deliberately excluded to focus on the subtle aspects of disc disruption and herniation.

RESULTS

Mechanical Behavior

The video recordings showed that after imposing the predetermined flexion the applied compression induced a forward displacement (Figure 2A, B) of the superior vertebra that was approximately equal in magnitude to that of the axial compressive displacement (Table 1). Also, just prior to disc failure, a faint definition of oblique fibers tilted toward the direction of the anterior shear was observed in the lateral disc periphery (see dashed box in Figure 2B), whereas this was not observed after the imposition of flexion only (see dashed box in Figure 2A). Furthermore, although only one lateral side was imaged, it was observed in 8 of the 14 tests that even without there being any externally visible evidence of disc damage, an audible tearing sound coincided with a sudden transient disturbance or ripple in the outer wall of the lateral annulus (see Video, Supplemental Digital Content 1, http://links.lww.com/BRS/B271, which demonstrates a faint ripple in the lateral annulus during the compression

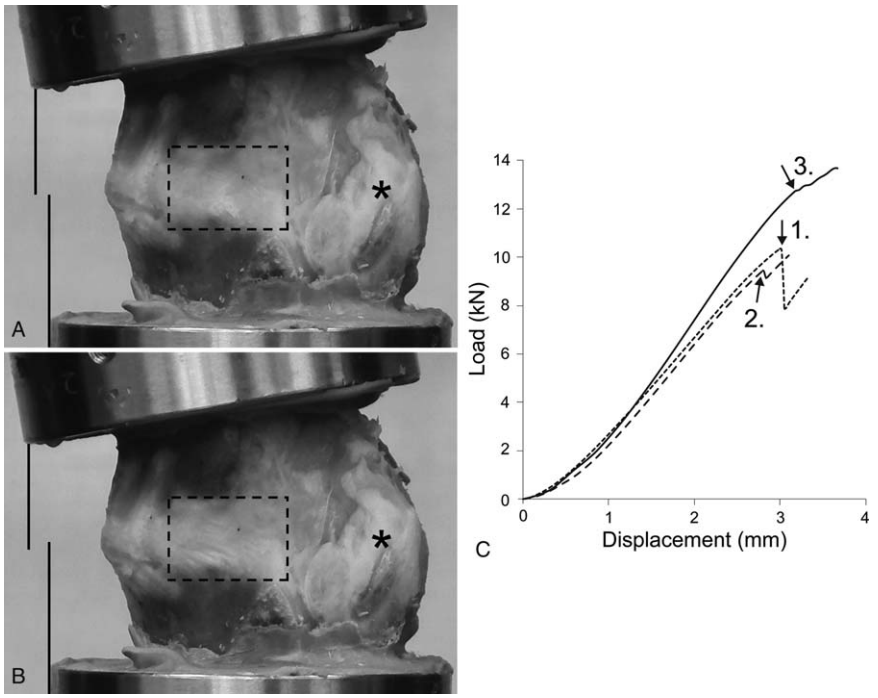

Figure 2. Mechanical response of motion segment. Images (**A**) and (**B**) show the motion segment from a lateral view with the anterior of the disc to the left. The facet joint (see asterisks) is obscured by soft tissue. **A**, Motion segment in flexed posture but still uncompressed. **B**, Compressed motion segment just prior to failure. A comparison of the vertical and horizontal positions of the tips of the black reference lines in (**A**) and (**B**) indicates that the applied axial compression also induced a degree of anterior shear of the superior vertebra. Also, inspection of the lateral wall in the boxed region in (**A**) indicated that with flexion only, no clear fiber alignment is visible, whereas following compression a faint taut, alignment of the oblique fibers tilted in the direction of anterior shear was visible (see box in **B**). **C**, Examples of load-displacement curves following the imposition of flexion and the corresponding points of initial failure (see arrows) which either coincided with the maximum load value before a visible drop, either large (1) or small (2), or with a subtle discontinuity (3).

TABLE 1. Summary of Mechanical and Structural Data

Disruption Category	Motion Segment (Spine-Disc Level)	Mechanical Data			Structural Data According to Mode of Disruption		Shown in Figure
		Forward Displacement of Superior Vertebra (mm)	Displacement Ratio: Forward ÷ Downward	Load at Initial Failure (kN)	Location of Radial Rupture	Location of Annular Disruption and Indication of Circumferential Tracking (+T)	
i	S1-L56	1.0	0.91	7.5	PL + NE	–	3A
	S2-L56	1.5	1.15	10.6	P + NE	–	3B
ii	S3-L12	1.1	1.10	8.7	P + B	1L + T	4A–C
	S4-L56	0.6	1.00	6.9	P + B	2L + T	–
iii	S5-L56	1.0	1.11	5.8	1L → L/ PL + NE	–	–
iv	S6-L34	0.9	1.29	7.2	–	1L + T	5A, B
	S7-L34	0.8	0.62	9.7	–	1L + T	–
	S5-L34	0.9	0.82	9.1	–	1L + T	–
	S8-L34	1.0	1.00	11.4	–	1L + T	–
	S9-L12	1.0	0.56	7.4	–	1L + T: 1L → P+B	6A–D
v	S10-L12	1.0	0.83	8.2	–	2L + T	7A–C
	S5-L12	1.1	1.00	7.9	–	2L + T	–
	S11-L56	1.3	1.30	7.8	–	2L + T: 1L → L/PL + NE	–
vi	S12-L34	1.1	0.85	12.8	–	A+T	–
Average	N/A	1.0	0.97	8.6	N/A	N/A	N/A

Modes of disruption are indicated by the transverse location and reported when externally visible by either focal bulging (+B) or nuclear extrusion (+NE). An externally visible herniation that initiated internally at a different location is further indicated by: begin → end locations.

1L indicates one lateral side; 2L, both lateral sides; A, anterior; B, focal bulging; L, lateral; N/A, not applicable, NE, nuclear extrusion; P, posterior; PL, posterolateral; T, circumferential tracking.

test) but without resulting in any obvious change in the lateral disc periphery following the removal of the applied compression.

The initial audible indication of disc failure in eight samples corresponded with the maximum load attained before a sudden drop in the load-displacement curve, either large or small (see curves 1, 2 in Figure 2C). For the remaining six samples initial failure was manifested as a subtle discontinuity in the load-displacement curve (see curve 3). Discs failed at an average load of 8.6 kN (Table 1), and there was no significant difference in mean initial failure load between the three spinal levels tested ($P > 0.05$).

Structural Response

The following six categories describe the different modes of disruption observed:

(i) Two discs failed *via* a direct radial rupture only, either posterolaterally or posteriorly, both resulting in uncontained nuclear extrusion (Figure 3A, B).

(ii) Two discs exhibited focal posterior bulging, i.e., contained herniations (Figure 4A). In both cases this bulging was a direct consequence of posterior radial rupture (Figure 4B). In one of these discs there was also clear evidence of nucleus penetrating into the mid-annulus at one lateral side and then tracking circumferentially within the layers causing a large inwards-distorting bulge (Figure 4C). In the second disc, nucleus penetrated both lateral sides. On one lateral side there was nuclear penetration into the mid annulus, similar to that in Figure 4C; on the other side the nucleus had penetrated into the inner lateral annulus and then tracked circumferentially

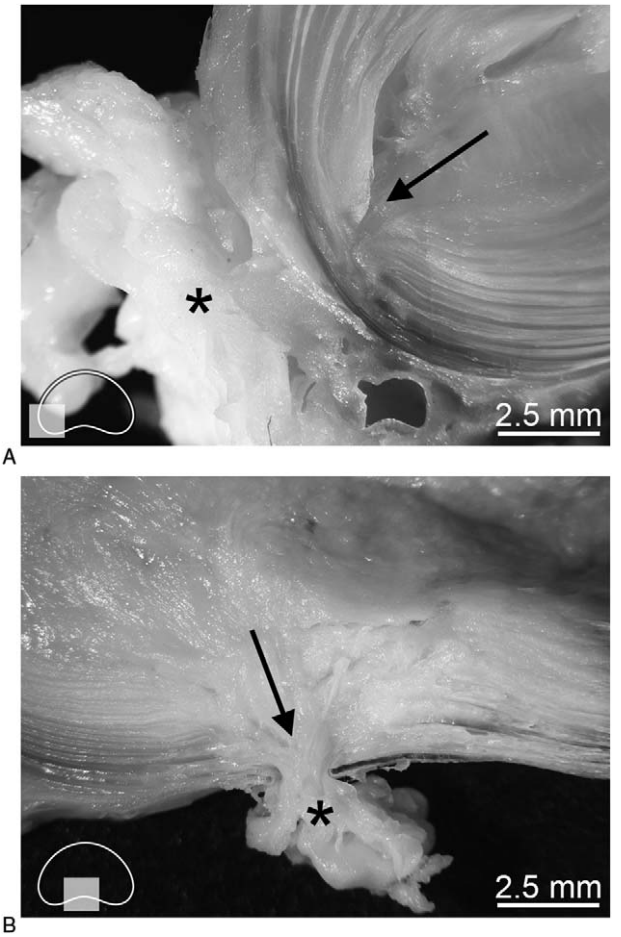

Figure 3. Images of two category (i) discs that failed only *via* direct radial rupture. In (**A**) herniation occurred *via* a posterolateral direct radial rupture, and in (**B**) as a posterior herniation as viewed in a transection. Both radial ruptures (see arrows) resulted in an uncontained extrusion of nuclear material (see asterisks).

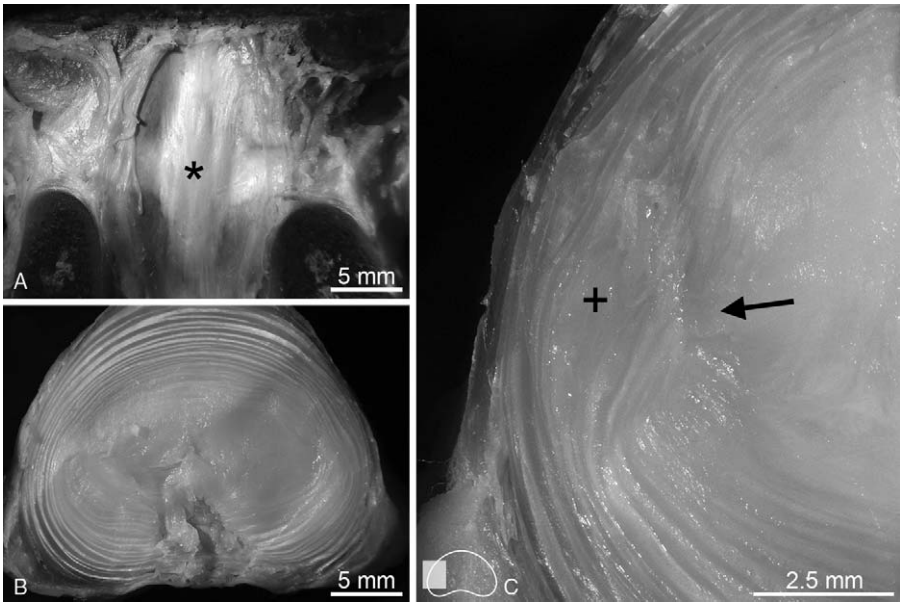

Figure 4. Representative images of the two category (ii) discs containing both disruption at the lateral annulus and a direct radial rupture at the posterior. Images (**A–C**) are from one of these discs with its externally visible ''contained'' herniation at the posterior (see asterisk in **A**) resulting from a direct posterior radial rupture as revealed by transverse sectioning (see **B**). Image (**C**) shows how nucleus has also penetrated into the mid lateral annulus (arrow) and then tracked circumferentially within the annulus to create a large inwards-distorting bulge between layers (see plus sign).

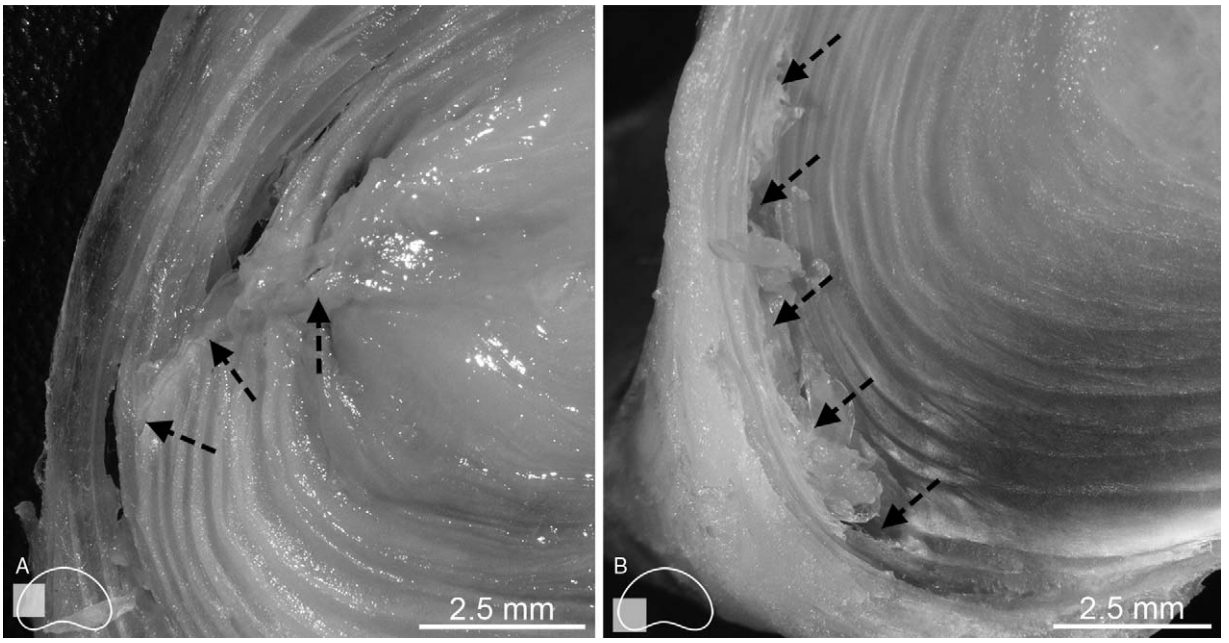

Figure 5. Example of category (iv) damage in a disc suffering lateral annular disruption of one side. Nuclear material penetrated the mid-to-outer lateral annulus and then deflected posterolaterally (see dashed arrows in **A**). Transverse sectioning of this same disc but at a different depth, combined with gentle probing, indicated that nuclear material had then tracked circumferentially deep into the posterolateral aspect (see dashed arrows in **B**).

posterolaterally some distance without further radial penetration.

(iii) One disc had a clear lateral disruption at one side which propagated as a skewed radial rupture leading to an uncontained nuclear extrusion at the lateral-posterolateral site.

(iv) In five discs, progressive transverse sectioning revealed a complete absence of any direct radial rupture. Instead, all in this group exhibited a similar pattern of annular disruption at one lateral side followed by circumferential nuclear tracking between lamellae to the posterolateral aspect. Figure 5 provides an example of this general pattern of failure. In Figure 5A nuclear material can be seen to migrate focally into the mid-to-outer lateral annulus (*i.e.*, fully contained) and then deflect posterolaterally (see dashed arrows). Gentle probing of another transverse section from the same disc but taken at a different depth is shown in Figure 5B and indicates that the nuclear material had tracked deep into the posterolateral aspect as indicated by the sequence of dashed arrows.

One of the above five category (iv) discs exhibited a contained posterior herniation (Figure 6A). Progressive transverse sectioning found no evidence of any direct nuclear penetration radially into the posterior bulge (Figure 6B, D), the only site of penetration being the lateral inner annulus (Figure 6B, C). Nuclear material was also found between the outer lamellae in the posterior-posterolateral annulus (see dashed arrows in Figure 6D) thus indicating that the contained posterior herniation (see asterisks) has resulted from nuclear material tracking circumferentially down from the site of lateral disruption.

(v) Three discs suffered disruptions at both lateral sides and in all three cases nuclear material tracked circumferentially within the annular layers toward the posterolateral aspect. The bilateral damage in one of these discs is shown in Figure 7A, B. At one lateral side nuclear material penetrated into the inner-to-mid annulus (see solid arrow in Figure 7B) where it then deflected posterolaterally (see dashed arrow in Figure 7B). The series of dashed arrows in Figure 7C identify the trail of nuclear material that has tracked circumferentially from the other lateral disruption shown in Figure 7A, eventually reaching as far as the dashed arrow in Figure 7A. The loose nuclear material in the posterolateral-lateral region shown in Figure 7C has been lifted out from between the annular layers by gentle probing.

In one of the three discs in this group, the nuclear material that penetrated the lateral annulus tracked circumferentially between the lamellae to the lateral-posterolateral outer annulus where it breached the disc to become externally visible.

(vi) One disc showed disruption of the inner annulus at the anterior aspect followed by circumferential tracking of nuclear material between lamellae. There were also minor disruptions found in the mid-to-outer lateral and posterolateral annulus. There was no evidence of any significant disruption of the inner

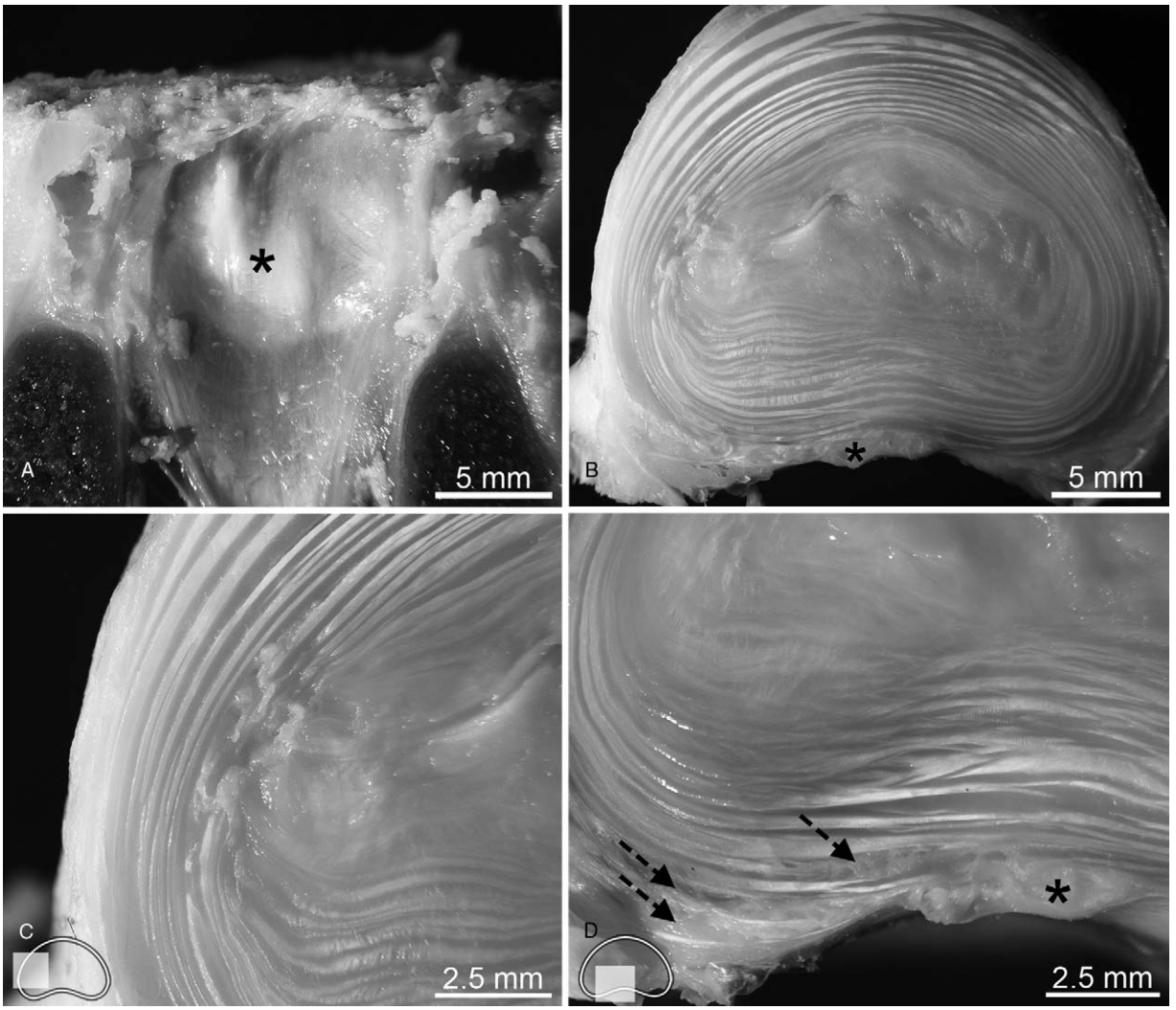

Figure 6. Disc with category (iv) damage showing a contained posterior herniation (see asterisks) imaged externally in (**A**) and in transectioned views in (**B**) and (**D**). Also note the disruption in the lateral annulus visible in (**B**) and enlarged in (**C**) but no evidence of any direct radial penetration of nucleus through the posterior annulus (see **B** and **D**). Dashed arrows in (**D**) identify nuclear material in the outer posterior-posterolateral annulus indicating that the contained posterior herniation (asterisk) has arisen from nuclear material tracking circumferentially down from the site of lateral disruption shown in (**B**) and (**C**).

annular layers in the lateral regions, suggesting that the nuclear material may have tracked from the anterior inner annulus disruption.

Finally, in all cases in which lateral disruption occurred (*i.e.*, 11 out of the 14 discs analyzed) there was no visible evidence of external bulging of the outer annulus immediately adjacent to these lateral sites. Also, at the level of structural resolution employed, there was no evidence of cartilaginous endplate material being associated with the nuclear material that had migrated specifically from the lateral annulus.

DISCUSSION

The use of an ovine lumbar model has the major advantage of providing an adequate number of healthy motion segments, a requirement that would have been difficult to meet had a human model been employed. Also, it is widely accepted that the ovine lumbar spine does provide a reasonable model for investigating aspects relevant to the human lumbar spine because of its similar anatomy,[32–34] biochemistry,[33] and biomechanics.[35]

Previously Adams and Hutton,[10] employing *in vitro* testing, demonstrated a higher incidence of herniation in human grade 2[36] discs (slightly degenerate) compared to grade 1 discs (healthy), arguing that degeneration is an important but not crucial factor. They explained the increased vulnerability of the slightly degenerate discs as arising from the combination of a still hydrostatic nucleus that can then break through the now weakened, stretched posterior annulus. Although we know that healthy ovine discs can be made to herniate,[20,21] whether mild degeneration similarly increases their vulnerability would be an interesting topic for further investigation if a reliable source of mildly degenerate ovine spines were available.

The 10° of flexion was chosen both because it lies within the range of physiological, nondamaging flexion for the

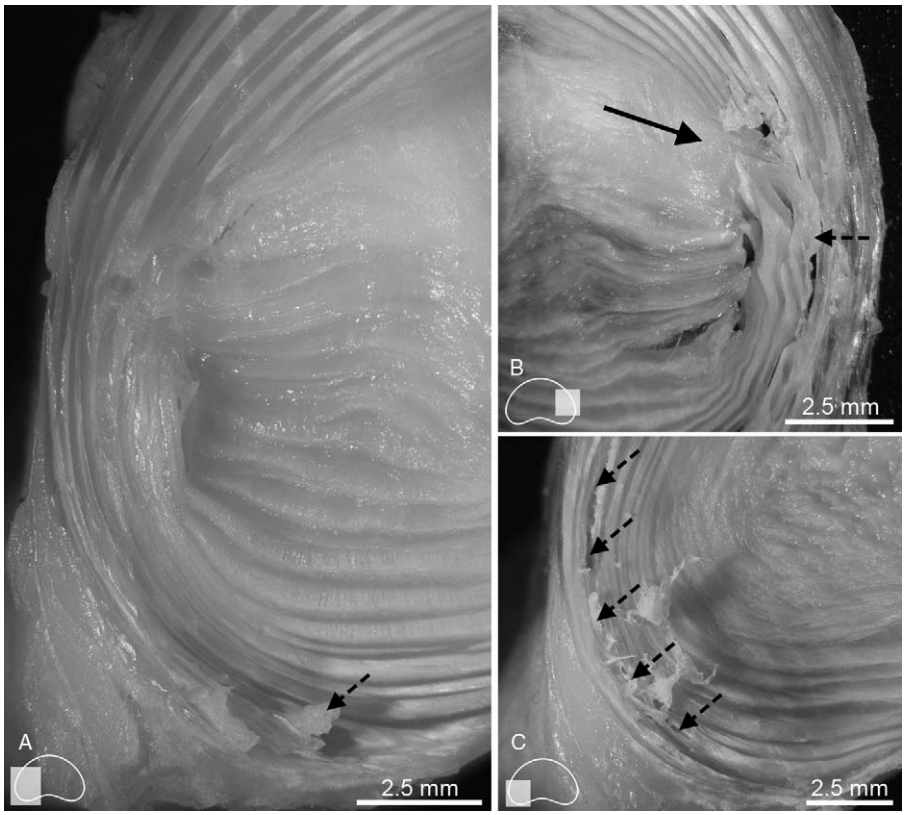

Figure 7. Disc with category (v) damage showing annular disruptions and nuclear penetration at both lateral sides (see **A** and **B**). Note that at the lateral site shown in (**B**) the nuclear material that has breached the inner-to-mid annulus (see solid arrow) has then been deflected posterolaterally (see dashed arrow). Progressive transverse sectioning of the other lateral site revealed that nuclear material had tracked circumferentially (see dashed arrows in **C**) deep into the posterolateral aspect (see also dashed arrow in **A**). Note that the loose nuclear material in the posterolateral-lateral region shown in (**C**) has been lifted out from between the annular layers by gentle probing.

ovine lumbar spine and, importantly, is also sufficient to achieve disc herniations *in vitro*.[18,20] Furthermore, 10° lies between the flexion angles measured in each level of the lumbar spine (ranging between 8° and 14°) in an average healthy human when moving from a standing posture to full flexion.[10,37]

The mean failure load of 8.6 kN obtained in the present study is not significantly different ($P > 0.05$) from the previously reported 8.9 kN for herniated discs using the same ovine model and testing conditions.[20] It should be noted that the latter study focused on the importance of the endplate profile and utilized sagittal sections confined to the posterior and posterolateral aspects of the disc for microstructural analysis. In contrast, we have used progressive transverse sectioning of the whole disc. So while our analysis is confined to the macro level, the more global picture of disruption obtained has revealed a herniation pathway that commences in the lateral annulus with the nuclear material then tracking circumferentially to become externally evident in the more generally acknowledged posterolateral and posterior herniation regions (Figure 6).

In all of our tests this lateral disruption did not cause any discernible external alteration in the lateral disc periphery following the removal of load. Clinically, discs appearing externally normal but containing an internal disruption causing low back pain are described by the pathologic entity *internal disc disruption*.[1,2] Therefore the initial lateral disruption and circumferential tracking of nuclear material that we have observed in our discs may well relate to a mode of internal disc disruption found during discography (Dallas Discogram Description[38]: grade 4[1,39]) if it is assumed that the clinically imaged circumferential contrast is in fact nuclear material.

Using internal pressurization of ovine motion segments in a neutral posture *in vitro*, Veres *et al*[16,19] reported, based on computed tomography imaging, that when the radiopaque gel penetrated the inner annulus at the anterior, lateral, or posterolateral aspects it then tracked circumferentially within the lamellae. Furthermore, two of their discs revealed that circumferential tracking of the injected gel from the anterior or lateral inner annulus was the primary pathway that appeared at the posterolateral or posterior disc periphery without the observation of endplate disruption.[16] These findings, based on a more global view of damage obtained using computed tomography imaging of the whole disc, are largely consistent with the results of the present study in which the circumferential tracking of nuclear material was a common occurrence. We note too that the transient disturbance (recorded by video, http://links.lww.com/BRS/B271) in the lateral wall is consistent with the internal lateral annular disruption clearly documented from our transverse sections (*e.g.*, Figures 4C and 5).

The high prevalence of lateral annulus disruption (11 discs out of 14 tested; Table 1) obtained in the present study indicates that it is the lateral margins of the disc that are highly vulnerable under the mechanical conditions employed.

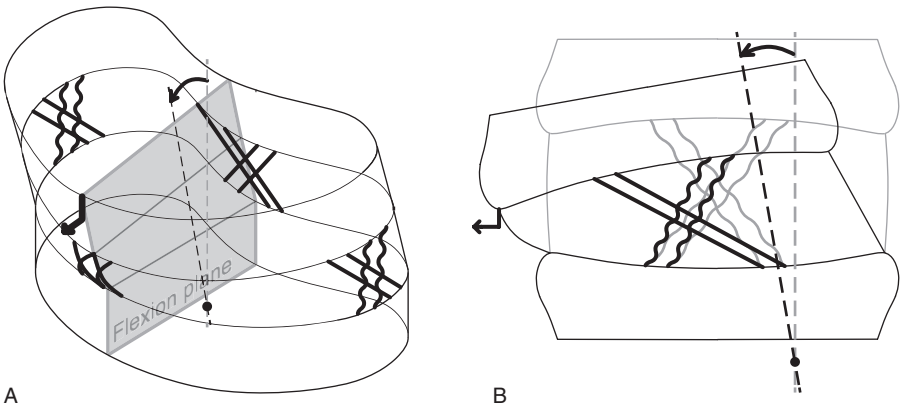

Figure 8. Schematics illustrating how anterior shear arising from combined flexion and compression influences the local response of the annular fibers. Schematic (**A**) illustrates how the oblique and counteroblique fiber sets in the anterior and posterior regions are recruited approximately evenly but not so in the lateral regions. Schematic (**B**) compares the neutral *versus* the flexed and compressed posture in the lateral annulus showing that anterior shear will increase the loading on those oblique fibers tilted in the direction of forward displacement but relax those in the counteroblique orientation.

So why does lateral disruption appear so frequently in our flexed, compressed discs?

The imposition of flexion induced a forward displacement of the superior vertebra (Figure 2A) as is known to occur in the upper levels of the lumbar spine when flexed *in vivo*.[37] This is due to the center of rotation being located slightly posteriorly and within the inferior vertebral body.[40,41] The present study has also shown that compression of the flexed motion segments up to the first indication of failure induced approximately equal amounts of forward and downward displacement (Table 1). Therefore a more complete mechanism of disc disruption under the combined influence of flexion and compression will most likely need to incorporate this anterior shear component.

The combined influence of anterior shear and flexion on disc failure has been discussed by Yingling and McGill.[42] In their *in vitro* study, pig cervical discs were loaded in anterior shear until failure in a neutral or 10° flexed posture. While acknowledging that their predominantly shear mode of loading may be uncommon *in vivo*, their neutral posture tests resulted in fractures across the pars interarticularis but with added flexion they also observed endplate avulsions in the lateral aspects. This would indicate that with the addition of flexion the annular fibers in these lateral regions are stressed to a level sufficient to create such avulsions.

Theoretical models representing the annulus[42] or disc[43] predict that anterior shear causes most deformation of the fibers in the lateral region. More important, anterior shear results in either an increase or decrease in the lateral fiber strains depending on the inclination of the fiber, whereas only minor changes are found for the anterior and posterior fibers.[43] Thus, anterior shear increases the loading on those oblique fibers tilted in the direction of forward displacement as seen in the lateral disc periphery just prior to failure (Figure 2B) but relax those in the counteroblique orientation. This differential recruitment means that the annular loading in these lateral regions is being carried primarily by only half of the annular layers.[42]

When considering the mechanical conditions employed in the present study the applied flexion, compression, and induced anterior shear will inevitably increase the loading in the posterior and anterior annulus. However, the oblique and counteroblique fiber sets in these two regions will be near-equally exposed to this loading because of their similar orientation in relation to the direction of anterior shear (Figure 8A). Conversely, in the lateral regions the anterior shear will result in an uneven recruitment of the oblique and counteroblique fibers sets (Figure 8A, B). With the increasing hydrostatic nuclear pressure acting on the annulus this uneven recruitment will increase the vulnerability to disruption of these lateral regions. This is consistent with the high incidence of lateral disruption reported in the present study.

Despite our observation of relatively high levels of disruption in the lateral annulus, there was little evidence to suggest that this led to lateral nuclear extrusions *via* direct radial rupture. It is entirely possible that the extensive circumferential tracking of nuclear material from the lateral regions reflects a path of lesser resistance created by intra-annular weakening, this in turn arising from the uneven recruitment of the oblique/counteroblique fiber sets.

The fact that herniations, both contained and extruded, mainly appear externally at the posterior or posterolateral annulus, suggests that these two sites are more susceptible to breaching of the *outer* annulus. Therefore our findings highlight the importance of performing a systematic structural analysis that yields a more global view of the patterns of disc disruption and movement of nuclear material.

Interestingly, in none of our discs was there any evidence of cartilaginous endplate being attached to the nuclear material that had migrated from the lateral annulus. The present study is therefore potentially relevant to patients who have acute sciatica due to nerve root inflammation and compression but who, through treatment, have rapid resolution of the inflammatory process and a diminution of herniation size.[44,45] This process would intuitively occur more rapidly where there was ''pure'' nucleus migration to the disc periphery as we have seen in the present study. In contrast, herniated material that contains annulus, and in particular the ''harder'' cartilaginous endplate, may well be less likely to resolve clinically and require surgical removal to relieve nerve root pressure.[46–48]

➢ Key Points

- ❑ Analysis of serial transverse sections systematically throughout the full volume of the disc provides a more complete picture of both the site of initial disruption and the herniation pathway.
- ❑ The present study revealed an additional herniation pathway that commences in the lateral annulus and which, *via* circumferential nuclear tracking, can become externally evident in the more generally recognized herniation regions, namely the posterolateral and posterior aspects.
- ❑ The vulnerability of the lateral annulus to disruption is thought to arise from the overloading of the differentially recruited oblique/counteroblique fiber sets as a consequence of the anterior shear developed in the flexed, compressed motion segment.
- ❑ The present study describes a newly identified herniation pathway and highlights the complex nature of the mechanisms leading to actual disc herniation.

Acknowledgments

The first author (V.M.vH) gratefully acknowledges Medtronic Australasia for funding her doctoral scholarship.

Supplemental digital content is available for this article. Direct URL citations appearing in the printed text are provided in the HTML and PDF version of this article on the journal's Web site (www.spinejournal.com).

References

1. Schwarzer AC, Aprill CN, Derby R, et al. The prevalence and clinical features of internal disc disruption in patients with chronic low back pain. *Spine (Phila Pa 1976)* 1995;20:1878–83.
2. Crock HV. Internal disc disruption. A challenge to disc prolapse fifty years on. *Spine (Phila Pa 1976)* 1986;11:650–3.
3. Inoue G, Ohtori S, Aoki Y, et al. Exposure of the nucleus pulposus to the outside of the annulus fibrosus induces nerve injury and regeneration of the afferent fibers innervating the lumbar intervertebral discs in rats. *Spine (Phila Pa 1976)* 2006;31:1433–8.
4. Palmgren T, Grönblad M, Virri J, et al. An immunohistochemical study of nerve structures in the annulus fibrosus of human normal lumbar intervertebral discs. *Spine (Phila Pa 1976)* 1999;24:2075–9.
5. Cavanaugh JM, Ozaktay AC, Yamashita T, et al. Mechanisms of low back pain: a neurophysiologic and neuroanatomic study. *Clin Orthop Relat Res* 1997;166–80.
6. Bogduk N, Tynan W, Wilson AS. The nerve supply to the human lumbar intervertebral discs. *J Anat* 1981;132:39–56.
7. Malinský J. The ontogenetic development of nerve terminations in the intervertebral discs of man (histology of intervertebral discs, 11th communication). *Cells Tissues Organs* 1959;38:96–113.
8. Roofe PG. Innervation of annulus fibrosus and posterior longitudinal ligament: fourth and fifth lumbar level. *Arch Neurol Psychiatry* 1940;44:100–3.
9. Porchet F, Wietlisbach V, Burnand B, et al. Relationship between severity of lumbar disc disease and disability scores in sciatica patients. *Neurosurgery* 2002;50:1253–60.
10. Adams MA, Hutton WC. Prolapsed intervertebral disc: a hyperflexion injury. *Spine (Phila Pa 1976)* 1982;7:184–91.
11. Adams MA, Hutton WC. The mechanics of prolapsed intervertebral disc. *Int Orthop* 1982;6:249–53.
12. McNally DS, Adams MA, Goodship AE. Can intervertebral disc prolapse be predicted by disc mechanics? *Spine (Phila Pa 1976)* 1993;18:1525–30.
13. Yoganandan N, Maiman DJ, Pintar F, et al. Microtrauma in the lumbar spine: a cause of low back pain. *Neurosurgery* 1988;23:162–8.
14. Lin HS, Liu YK, Adams KH. Mechanical response of the lumbar intervertebral joint under physiological (complex) loading. *J Bone Joint Surg Am* 1978;60A:41–55.
15. Brown T, Hansen RJ, Yorra AJ. Some mechanical tests on the lumbosacral spine with particular reference to the intervertebral discs. *J Bone Joint Surg* 1957;39:1135–64.
16. Veres SP, Robertson PA, Broom ND. ISSLS prize winner: how loading rate influences disc failure mechanics: a microstructural assessment of internal disruption. *Spine (Phila Pa 1976)* 2010;35:1897–908.
17. Veres SP, Robertson PA, Broom ND. The influence of torsion on disc herniation when combined with flexion. *Eur Spine J* 2010;19:1468–78.
18. Veres SP, Robertson PA, Broom ND. The morphology of acute disc herniation: a clinically relevant model defining the role of flexion. *Spine (Phila Pa 1976)* 2009;34:2288–96.
19. Veres SP, Robertson PA, Broom ND. ISSLS prize winner: microstructure and mechanical disruption of the lumbar disc annulus: part II: how the annulus fails under hydrostatic pressure. *Spine (Phila Pa 1976)* 2008;33:2711–20.
20. Wade KR, Robertson PA, Thambyah A, et al. How healthy discs herniate: a biomechanical and microstructural study investigating the combined effects of compression rate and flexion. *Spine (Phila Pa 1976)* 2014;39:1018–28.
21. Wade KR, Robertson PA, Thambyah A, et al. "Surprise" loading in flexion increases the risk of disc herniation due to annulus-endplate junction failure. *Spine (Phila Pa 1976)* 2015;40:891–901.
22. Ebeling U, Reulen HJ. Are there typical localisations of lumbar disc herniations? A prospective study. *Acta Neurochir (Wien)* 1992;117:143–8.
23. Knop-Jergas BM, Zucherman JF, Hsu KY, et al. Anatomic position of a herniated nucleus pulposus predicts the outcome of lumbar discectomy. *J Spinal Disord* 1996;9:246–50.
24. Maezawa S, Muro T. Pain provocation at lumbar discography as analyzed by computed tomography/discography. *Spine (Phila Pa 1976)* 1992;17: 1309–15.
25. Ninomiya M, Muro T. Pathoanatomy of lumbar disc herniation as demonstrated by computed tomography/discography. *Spine (Phila Pa 1976)* 1992;17:1316–22.
26. Schmidt H, Bashkuev M, Dreischarf M, et al. Computational biomechanics of a lumbar motion segment in pure and combined shear loads. *J Biomech* 2013;46:2513–21.
27. Sharma M, Langrana NA, Rodriguez J. Role of ligaments and facets in lumbar spinal stability. *Spine (Phila Pa 1976)* 1995;20:887–900.
28. Adams MA, Hutton WC. The mechanical function of the lumbar apophyseal joints. *Spine (Phila Pa 1976)* 1983;8:327–30.
29. Costi JJ, Hearn TC, Fazzalari NL. The effect of hydration on the stiffness of intervertebral discs in an ovine model. *Clin Biomech* 2002;17:446–55.
30. Simunic DI, Broom ND, Robertson PA. Biomechanical factors influencing nuclear disruption of the intervertebral disc. *Spine (Phila Pa 1976)* 2001;26:1223–30.
31. Pflaster DS, Krag MH, Johnson CC, et al. Effect of test environment on intervertebral disc hydration. *Spine (Phila Pa 1976)* 1997;22:133–9.
32. Brown S, Rodrigues S, Sharp C, et al. Staying connected: structural integration at the intervertebral disc–vertebra interface of human lumbar spines. *Eur Spine J* 2017;26:248–58.
33. Reid JE, Meakin JR, Robins SP, et al. Sheep lumbar intervertebral discs as models for human discs. *Clin Biomech* 2002;17:312–4.

34. Wilke HJ, Kettler A, Wenger KH, et al. Anatomy of the sheep spine and its comparison to the human spine. *Anat Rec* 1997;247:542–55.
35. Wilke HJ, Kettler A, Claes LE. Are sheep spines a valid biomechanical model for human spines? *Spine (Phila Pa 1976)* 1997;22:2365–74.
36. Galante JO. Tensile properties of the human lumbar annulus fibrosus. *Acta Orthop Scand* 1967;1–91.
37. Pearcy M, Portek I, Shepherd J. Three-dimensional x-ray analysis of normal movement in the lumbar spine. *Spine (Phila Pa 1976)* 1984;9:294–7.
38. Sachs BL, Vanharanta H, Spivey MA, et al. Dallas discogram description. A new classification of Ct/discography in low-back disorders. *Spine (Phila Pa 1976)* 1987;12:287–94.
39. Aprill BC, Bogduk N. High-intensity zone: a diagnostic sign of painful lumbar disc on magnetic resonance imaging. *Br J Radiol* 1992;65:361–9.
40. Yoshioka T, Tsuji H, Hirano N, et al. Motion characteristic of the normal lumbar spine in young adults: instantaneous axis of rotation and vertebral center motion analyses. *J Spinal Disord* 1990;3:103–13.
41. Pearcy MJ, Bogduk N. Instantaneous axes of rotation of the lumbar intervertebral joints. *Spine (Phila Pa 1976)* 1988;13:1033–41.
42. Yingling VR, McGill SM. Anterior shear of spinal motion segments: kinematics, kinetics, and resultant injuries observed in a porcine model. *Spine (Phila Pa 1976)* 1999;24:1882–9.
43. Broberg KB. On the mechanical behaviour of intervertebral discs. *Spine (Phila Pa 1976)* 1983;8:151–65.
44. Vialle LR, Vialle EN, Henao JES, et al. Hérnia discal lombar. *Rev Bras Ortop* 2010;45:17–22.
45. Ghahreman A, Bogduk N. Predictors of a favorable response to transforaminal injection of steroids in patients with lumbar radicular pain due to disc herniation. *Pain Med* 2011;12:871–9.
46. Joe E, Lee JW, Park KW, et al. Herniation of cartilaginous endplates in the lumbar spine: MRI findings. *Am J Roentgenol* 2015;204:1075–81.
47. Lama P, Zehra U, Balkovec C, et al. Significance of cartilage endplate within herniated disc tissue. *Eur Spine J* 2014;23:1869–77.
48. Willburger RE, Ehiosun UK, Kuhnen C, et al. Clinical symptoms in lumbar disc herniations and their correlation to the histological composition of the extruded disc material. *Spine (Phila Pa 1976)* 2004;29:1655–61.